Photoluminescence spectroscopy of single silicon quantum dots

Jan Valenta,[a] Robert Juhasz, and Jan Linnros
Department of Microelectronics and Information Technology, Royal Institute of Technology, Electrum 229, 164 21 Kista-Stockholm, Sweden

(Received 9 October 2001; accepted for publication 13 December 2001)

Photoluminescence (PL) from single silicon quantum dots have been recorded and spectrally resolved at room temperature. The Si nanocrystals (NCs) were fabricated using electron-beam lithography and reactive ion etching resulting in Si nanopillars that were subsequently oxidized to produce luminescent silicon cores. The NCs are organized in a regular matrix which enables repeated observation of a specific single NC. By reflection and PL imaging, the emission is shown to originate from the Si nanopillars. The single-NC PL spectrum has a single band with a width of ~130 meV. The emission is polarized in arbitrary directions suggestive of geometrical differences in the shape of the nanocrystals. The quantum efficiency of the PL has been found to reach as much as 35% for some nanocrystals. Our experiments support the quantum-confinement model for the PL emission of Si nanocrystals and elucidate the critical role of defect passivation. © *2002 American Institute of Physics.* [DOI: 10.1063/1.1448400]

Semiconductor quantum dots (QDs) or nanocrystals (NCs) are potential building blocks of future nanoelectronics and nanophotonics. Among other materials, nanocrystalline silicon has attracted much interest after the discovery of strong photoluminescence (PL) emission from porous Si.[1] The PL mechanism in Si NCs has been intensively debated and several models proposed. Detailed studies are, however, hampered by the broad PL band resulting from inhomogeneous broadening, omnipresent in ensembles of NCs. Although certain improvement can be achieved by size-selection methods,[2] single-dot spectroscopy techniques would be needed to reveal the PL mechanism. These methods are widely applied to study individual NCs of III–V and II–VI semiconductors[3] but have only scarcely been used to study light emission from silicon NCs (Si NCs).[4,5] Two main difficulties are the low emission rate from the Si NC (long radiation lifetime resulting from the indirect transition) and the complicated preparation of diluted and well-defined systems of Si NCs. Recently, the Buratto group reported PL studies of dispersed single porous-Si grains.[4,6]

In this letter, we present single-dot PL spectra of individual Si NCs measured at room temperature (RT). We have taken an entirely different approach in isolating the NCs using electron-beam lithography and plasma etching to produce a regular matrix of Si pillars, followed by size reduction using subsequent two-stage oxidation. As a result, we are able to identify luminescing pillars, verify that the PL indeed originates from these structures, and determine the quantum efficiency of the PL. We also describe significant intensity fluctuations and polarization effects suggesting shape variations of NCs.

Electron-beam lithography was used to form resist dots with diameters as small as 50 nm on an *N*-type ($\langle 100 \rangle$, 20–40 Ω cm) Si wafer having a 25 nm thermal oxide layer. Reactive ion etching (RIE) using CHF_3/O_2-based chemistry was then performed to etch through the top SiO_2 layer followed by chlorine based RIE for Si etching. The resulting 200 nm tall pillars are shown by the scanning electron microcopy image (SEM) of Fig. 1(a) for nominal pillar diameters of 130 nm. The samples were subsequently thermally oxidized for 5 h in O_2 gas at 850 or 900 °C. The oxide was then removed by buffered wet etching and the samples imaged by SEM [Fig. 1(b)]. A second oxidation followed at 1000 °C for 12 min [Fig. 1(c)] in order to shrink the remaining Si cores even further. Finally, the samples were annealed for 30 min at 400 °C in a 1:9 mixture of $H_2:N_2$ gas to passivate the surface states in order to enhance the PL.

PL images and spectra of the Si NCs were studied using an imaging spectrometer connected to a conventional optical (far-field) microscope. The light emitted from a sample was collected by an objective, imaged on the entrance slit of the spectrometer, and detected at the output by a liquid-nitrogen-cooled charge-coupled-device camera. Reflection images were detected under illumination with the blue (442 nm) line of a cw He–Cd laser while the PL was excited by the UV line (325 nm) of the same laser. The laser beam impinged on the sample surface at grazing incidence. All spectra were corrected for the spectral sensitivity of the detection system.

Figure 2 [part (a)] presents a reflection image of a matrix of Si NCs made by oxidation of 100-nm-wide pillars. The PL

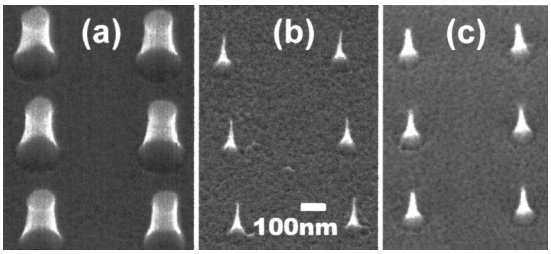

FIG. 1. SEM images (45° tilt view) of Si nanopillars after initial patterning (a), following size reduction by thermal oxidation and removal of oxide (b), and following the last oxidation step (c).

[a]Permanent address: Department of Chemical Physics and Optics, Charles University, Ke Karlovu 3, CZ-121 16 Prague 2, Czechia; electronic mail: valenta@karlov.mff.cuni.cz

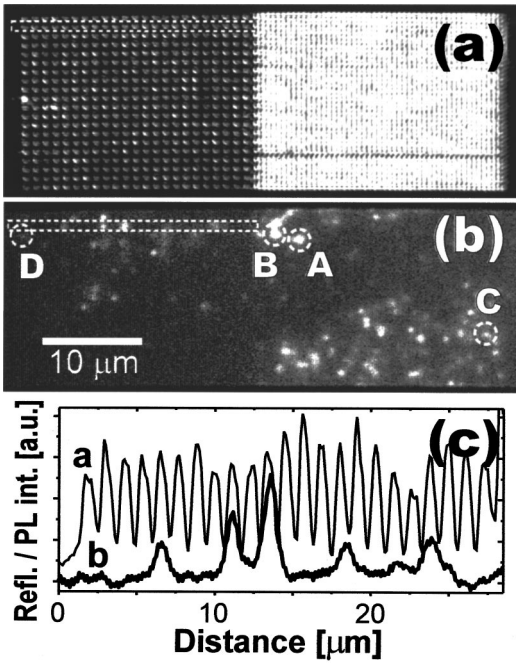

FIG. 2. Reflection (a) and PL (b) image of regular lattice of Si NCs. Distance between neighbor NCs is 1 and 0.5 μm for the left and right sides of the sample, respectively. Panel (c) compares intensity profiles of reflection (a) and PL (b) signal taken from the same part of sample [indicated by dashed rectangles in the left-upper corner of images (a) and (b)]. Circles in image (b) indicate NCs referred to in Figs. 3 and 4.

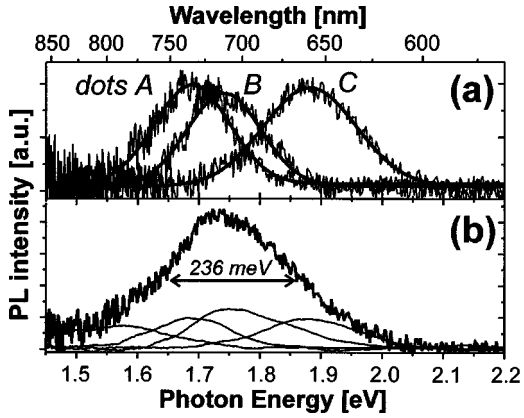

FIG. 3. PL spectra of three different single Si NCs under 325 nm excitation (0.5 W/cm^2) at RT [panel (a)]. Positions of these NCs in the sample are indicated by white circles in Fig. 2(b). The bold smooth lines are Gaussian fits (FWHM is 122, 120, and 152 meV for dots A, B, and C, respectively). Panel (b) shows a sum of nine spectra of different single NC from one sample. Four of these individual spectra (smoothed out) are shown under the sum spectrum.

image of the same part of the sample [Fig. 2(b)] reveals a small number of emitting Si NCs with various intensities. The intensity profiles of reflection and PL [Fig. 2(c)] show a very good coincidence of peak positions, indeed, a strong indication that the PL originates from individual pillars organized in a regular two-dimensional lattice. The spatial resolution of the detected images is restricted by diffraction, which gives the limit of about 500 nm in reflection and slightly worse in PL [see Fig. 2(c)]. However, we can often resolve the PL from individual pillars even in the case when the spacing is on the limit of resolution [0.5 μm—right-hand side of the Figs. 2(a) and 2(b)] because only a small fraction of the dots is shining.

PL spectra of individual Si NCs can be measured for the most intensively luminescing dots. In Fig. 3, we show the spectra of three dots. The detection time was 30 min at the excitation intensity of 0.5 W/cm^2, and the spectral resolution was about 10 nm. The PL spectrum is formed by a single band, which can be well fitted by a single Gaussian peak lying in the range 1.58–1.88 eV (660–785 nm). Results of fits are plotted by bold black lines in Fig. 3, yielding full width at half maximum (FWHM) values in the range 120–210 meV. The bottom part of Fig. 3 shows a sum of nine spectra of individual dots measured under identical conditions in one sample. As expected, this ensemble spectrum is significantly broader than individual spectra.

According to the experimental data of Wolkin *et al.*[7] and the calculations of Reboredo, Franceschetti, and Zunger,[8] a PL maximum at 1.7 eV corresponds to a NC diameter of about 3.6 nm. However, we are not yet able to confirm the size of the Si core of a luminescing single NC by direct measurement. The relatively large bandwidth of the PL spectrum (120–210 meV) is common for single NCs at RT (see, for example Ref. 9). It is mainly due to participation of one, two, or more phonons in optical transitions (the energy of LO phonon in the Γ point of bulk Si at RT is 64.4 meV). Other effects like the existence of several localized states in one Si NC, stress in a Si core, vibrations on the Si–SiO_2 interface, etc., could also contribute to the broadening of the PL spectrum. Therefore, it is desirable to measure the PL of a single Si NC also at low temperatures. Such experiments would be complicated as the PL photon rate is further reduced due to the longer lifetime of Si NC excited states.

Increasing the intensity of pumping broadens slightly the emission band of a single Si NC and the integrated PL intensity starts to saturate at intensities exceeding $\sim$0.2 W/cm^2. The saturation can be caused by two effects: Saturation of absorption (for an absorption cross section of 10^{-14} cm^{-1} and 0.1 ms lifetime,[10] the population of 1 exciton/NC will be reached with 0.8 W/cm^2 excitation) and PL intermittence (on–off blinking). The on–off switching (on the time scale of seconds and ms) is often observed in emission of single NCs and molecules and explained as a charging (photoionization) effect. With increasing excitation power the individual emitter stays a shorter time in the on state and the PL intensity saturates.[9]

The measurement of PL intermittence in our single Si NCs is restricted by the shortest detection time needed to obtain a reasonable signal-to-noise ratio, which is about 1 min. Despite this poor time resolution, we observed relatively large fluctuations of the PL intensity for certain NCs, whereas some NCs appear stable. This observation confirms a single-center origin of PL at least for some of the studied Si NCs. Details about the PL intensity dependence and fluctuations will be published separately.

Finally, we present polarization-sensitive detection of single NC PL using a linearly polarized laser beam and an analyzer inside a microscope. This configuration allows checking the projection of the emitting dipole in the plane parallel to the sample surface. The results shown in Fig. 4 indicate that the PL from a majority of individual QDs has a high degree of polarization. On the other hand, there is almost no polarization memory—i.e., the orientation of the PL

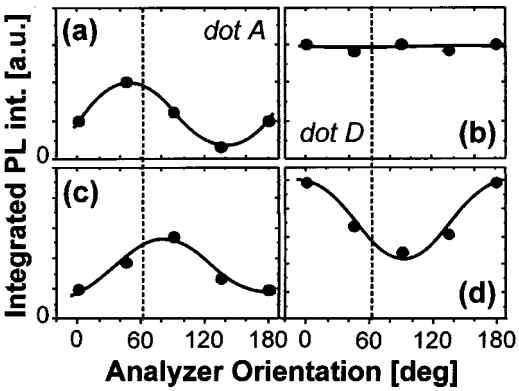

FIG. 4. Polarization selective detection of PL from single NCs: Integrated PL signal from dots A and D together with two other dots are plotted as a function of the analyzer orientation. Experimental dots are fitted with a squared sinusoid. The dashed lines mark the angle corresponding to projection of the laser-beam polarization.

polarization is independent of the exciting beam polarization (projected at $\alpha = 62°$). The high degree of polarization indicates that the orientation of an emitting dipole is quite stable. This suggests that NCs showing polarized PL are elongated in different directions,[11] whereas NCs with non polarized PL have either a random orientation of the emitting dipole (spherical shape) or the dipole is oriented perpendicularly to the sample surface. The absence of a polarization memory along with the high-energy relaxation between excitation and emission photon energy indicate that absorbing and emitting states may be very different.

The well-defined experimental conditions allow us to estimate the PL quantum efficiency for the best-emitting Si NCs. For an excitation intensity of $P = 80\ \mathrm{mW/cm^2}$ (i.e., $\sim 1.3\times 10^{17}$ photons/s/cm^2), and using an absorption cross section $\sigma \sim 1\times 10^{-14}$ cm^2,[10] the signal count rate, N, can be calculated using:

$$N = D\,\eta\sigma P, \tag{1}$$

where η is the PL quantum efficiency (QE) and D is the overall detection efficiency of photons emitted by a NC ($D = 0.026$ for our experimental setup). The most intense NCs produce count rates of ~ 12 counts/s under $P = 80\ \mathrm{mW/cm^2}$. This gives us a high QE of about 35% although the majority of dots seen in Fig. 2(b) have QEs between 5% and 20%.

Our results are in good agreement with the PL measurements of individual grains of porous Si by Buratto's group.[4,6] They found an even higher PL QE of 88% using the method of saturated count rate:

$$N_{\mathrm{sat}} = D\,\eta/\tau, \tag{2}$$

where τ is the excited-state lifetime. For the NC used in the above-described calculation, we found N_{sat} about 40 counts/s. Using $\tau = 100\ \mu s$, taken from measurements on the ensemble of Si NCs,[11] Eq. (2) yields a QE of 15%, which corresponds well with the value obtained from Eq. (1) for the highest excitation intensity we used. The excited-state lifetime may, however, be significantly different in the present structures.

Finally, let us note that only a few percent of Si NCs in our structures show detectable PL, cf. Fig. 2(b) (in Ref. 11, only $\sim 2.8\%$ of porous Si particles were luminescent). The reason could be nonradiative quenching by defects or escape of e–h pairs to the substrate. Indeed, the critical role of defect passivation was clearly illustrated by the fact that the PL was totally quenched following the electron-beam exposure during SEM imaging and could only be regained by a forming gas anneal. Therefore, better isolation of NCs from the substrate and different oxidation conditions and forming-gas anneals are clearly worth studying. The main advantage of our samples with a regular organization of NCs is the possibility to repeatedly retrieve and measure a specific single NC following different post-treatments of a sample. Whether it is possible to increase the fraction of luminescing dots and their QE, or, if the statistical nature of the occurrence of defects in NCs puts an upper limit to these numbers, remains unanswered.

In conclusion, we have prepared regular lattices of Si nanopillars that were oxidized to effectively result in oxide covered zero-dimensional Si nanocrystals and measured PL spectra of individual Si NCs at RT. The PL spectral positions are in agreement with previous measurements on ensembles of Si NCs and with theoretical works and the spectral width is clearly narrower than the ensemble spectra. The quantum efficiency of the PL in the best Si NCs was found to be about 35%. Finally, we have demonstrated PL intensity fluctuations and a high degree of emission polarization, suggesting charging effects and the nonspherical shape of the NCs, respectively.

The authors gratefully acknowledge discussions with S. Empedocles, A. Galeckas, N. Lalic, and M. Vácha, and the access to the e-beam lithography at Chalmers and at the KTH nanolab. Partial funding was received from the KTH Faculty and the European SBLED project. One of the authors (J.V.) acknowledges support from GAAV CR Project No. B1112901.

[1] A. G. Cullis, L. T. Canham, and P. D. J. Calcott, J. Appl. Phys. **82**, 909 (1997).
[2] W. L. Wilson, P. F. Szajowski, and L. E. Brus, Science **262**, 1242 (1993).
[3] A. Gustafsson, M.-E. Pistol, L. Montellius, and L. Samuelson, J. Appl. Phys. **84**, 1715 (1998).
[4] M. D. Mason, G. M. Credo, K. D. Weston, and S. K. Buratto, Phys. Rev. Lett. **80**, 5405 (1998).
[5] J. K. Rogers, F. Seiferth, and M. Vaez-Iravani, Appl. Phys. Lett. **66**, 3260 (1995).
[6] G. M. Credo, M. D. Mason, and S. K. Buratto, Appl. Phys. Lett. **74**, 1978 (1999).
[7] M. V. Wolkin, J. Jorne, P. M. Fauchet, G. Allan, and C. Delerue, Phys. Rev. Lett. **82**, 197 (1999).
[8] F. A. Reboredo, A. Franceschetti, and A. Zunger, Phys. Rev. B **61**, 13073 (2000).
[9] U. Banin, M. Bruchez, A. P. Alivisatos, T. Ha, S. Weiss, and D. S. Chemla, J. Chem. Phys. **110**, 1195 (1999).
[10] D. Kovalev, K. Heckler, G. Polisski, and F. Koch, Phys. Status Solidi B **215**, 871 (1999).
[11] J. Linnros, N. Lalic, A. Galeckas, and V. Grivickas, J. Appl. Phys. **86**, 6128 (1999).